

Steric Control of Oxygenation Regiochemistry in Soybean Lipoygenase-1

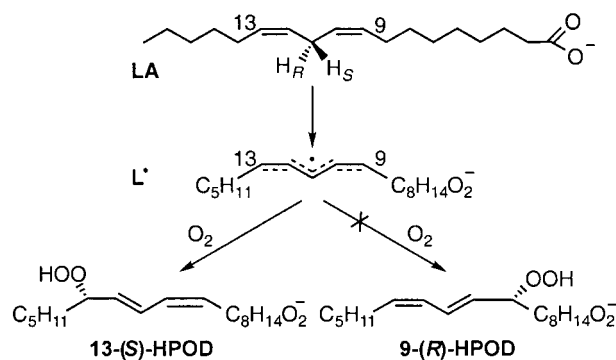
Michael J. Knapp, Florian P. Seebeck,[‡] and Judith P. Klinman*

Department of Chemistry, University of California Berkeley, California 94720

Received November 2, 2000

Mammalian lipoxygenases catalyze the formation of important biological secondary messengers and have been implicated in carcinogenesis¹ and inflammation.² While the catalytic reaction of all known lipoxygenases leads to the formation of a substrate-derived radical intermediate, most lipoxygenase products are highly regio- and stereopure.³ Soybean lipoxygenase-1 (SLO), the prototypical model lipoxygenase, catalyzes the oxidation of linoleic acid (LA) by O₂, producing 13-(*S*)-hydroperoxyoctadecadienoic acid (HPOD). The first chemical step in this reaction⁴ is abstraction of the pro-*S* hydrogen atom from C-11 by the active-site Fe³⁺-OH to generate a putatively delocalized carbon based radical (L[•]) and Fe²⁺-OH₂. This intermediate reacts with O₂ to regenerate Fe³⁺-OH and the product 13-(*S*)-HPOD (Scheme 1). Reactions in solution between carbon radicals and triplet O₂ typically lead to many isomers and are generally diffusion limited.⁵ While SLO reacts with O₂ at a rapid rate ($k_{\text{cat}}/K_{\text{M}}(\text{O}_2) = 4.4 \times 10^6 \text{ M}^{-1} \text{ s}^{-1}$), this reaction remains highly selective for O₂ attack at C-13. This has led to the notion that the active-site Fe²⁺ influences the site of O₂ insertion via a purple (Fe-OOL)²⁺ intermediate.¹⁸ However, this idea is difficult to reconcile with the fact that H-abstraction by Fe³⁺-OH is antarafacial to O₂ insertion.⁶ Inspection of the crystal structure for SLO⁷ reveals a

Scheme 1. Simplified Chemical Mechanism of SLO^a



^a WT-SLO produces predominantly 13-(*S*)-HPOD at high pH.

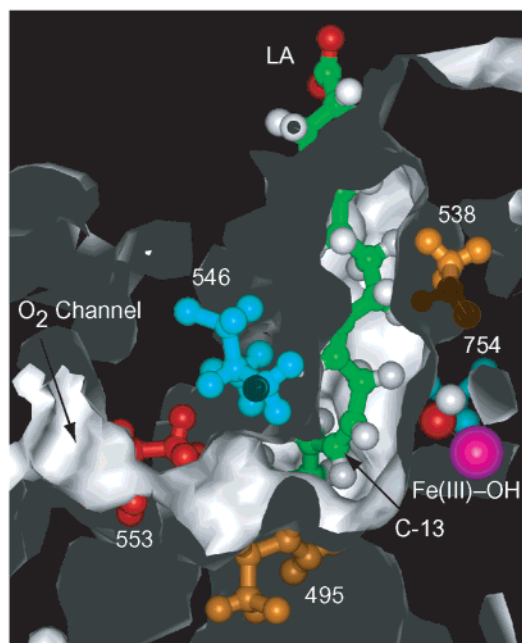


Figure 1. Substrate cavity and O₂ access channel of SLO shown as a white surface. The substrate LA (C, green; H, white; O, red) has been modeled with C-1 toward the top of the figure, and with the C-9–C-13 moiety of substrate between Ile⁵³⁸ and Gln⁴⁹⁵ (orange). The postulated O₂ channel, on top of Ile⁵⁵³ (red), intersects the substrate cavity close to the C-13 position of LA. Leu⁵⁴⁶ and Leu⁷⁵⁴ (blue) constrict the LA channel, preventing O₂ access to C-9 of LA. Fe³⁺-OH is presented as CPK spheres (Fe, magenta; O, red; H, white).¹⁶

side channel intersecting the substrate pocket near the reactive C-11, proposed⁷ to permit O₂ access. The current report details our investigation into the role played by bulky hydrophobic residues in controlling the regiospecificity of SLO. Steady-state kinetics and product distribution data from single-point mutants of SLO show that Leu⁵⁴⁶ and Leu⁷⁵⁴ grant selectivity for 13-(*S*)-HPOD by blocking O₂ access to C-9 of LA, and that O₂ enters the active site via the postulated side channel. These results indicate that SLO controls O₂ access to the intermediate L[•], and suggest that Fe²⁺ plays a secondary role in oxygenation.

The X-ray crystal structure of SLO revealed the LA pocket, cavity IIa,⁷ as a twisted channel, constricted at the Fe³⁺-OH by the side chains of Leu⁵⁴⁶ and Leu⁷⁵⁴ (Figure 1). A sharp bend near Fe³⁺-OH is introduced by the side chains of Gln⁴⁹⁵ and Ile⁵³⁸. On the basis of extensive experiments with many lipoxygenases^{8–13} models have been published^{6,10,11,13} describing substrate binding in which the reactive C-11 lies near the constriction formed by

[‡] Current address: Laboratory of Organic Chemistry, Swiss Federal Institute of Technology (ETH), CH-8092, Zürich, Switzerland.

- (1) Rioux, N.; Castonguay, A. *Carcinogenesis* **1998**, *19*, 1393–1400.
- (2) Samuelsson, B.; Dahlen, S.-E.; Lindgren, J.; Rouzer, C. A.; Serhan, C. N. *Science* **1987**, *237*, 1171–1176.
- (3) Kuhn, H.; Thiele, B. *J. FEBS Lett.* **1999**, *449*, 7–11.
- (4) Glickman, M. H.; Klinman, J. P. *Biochemistry* **1996**, *35*, 12882–12892.
- (5) Walling, C. Autoxidation. In *Active Oxygen in Chemistry*, 1st ed.; Foote, C. S., Valentine, J. S., Greenberg, A., Liebman, J. F., Eds.; Chapman and Hall: London, 1995; Vol. 2, pp 24–65.
- (6) Gardner, H. W. *Biochim. Biophys. Acta* **1989**, *1001*, 274–281.
- (7) Minor, W.; Steczko, J.; Stec, B.; Otwinowski, Z.; Bolin, J. T.; Walter, R.; Axelrod, B. *Biochemistry* **1996**, *35*, 10687–10701.
- (8) Schwarz, K.; Borngraber, S.; Anton, M.; Kuhn, H. *Biochemistry* **1998**, *37*, 15327–15335.
- (9) Jisaka, M.; Kim, R. B.; Boeglin, W. E.; Brash, A. R. *J. Biol. Chem.* **2000**, *275*, 1287–1293.
- (10) Gan, Q. F.; Browner, M. F.; Sloane, D. L.; Sigal, E. *J. Biol. Chem.* **1996**, *271*, 25412–25418.
- (11) Hornung, E.; Walth, M.; Kuhn, H.; Feussner, I. *Proc. Natl. Acad. Sci. U.S.A.* **1999**, *96*, 4192–4197.
- (12) Nelson, M. J.; Seitz, S. P. *Curr. Opin. Struct. Biol.* **1994**, *4*, 878–884.
- (13) Gillmor, S. A.; Villanor, A.; Fletterick, R.; Sigal, E.; Browner, M. F. *Nat. Struct. Biol.* **1997**, *4*, 1003–1009.
- (14) Holman, T. R.; Zhou, J.; Solomon, E. I. *J. Am. Chem. Soc.* **1998**, *120*, 12564–12572.
- (15) Rickert, K. W.; Klinman, J. P. *Biochemistry* **1999**, *38*, 12218–12228.
- (16) All modeling was performed using InsightII/Discover software (Biosym/MSI, San Diego, CA). The CVFF force field was used, and the pro-*S* hydrogen of LA was constrained to lie within 3.0 Å of the oxygen atom of Fe(III)-OH. Only residues within the substrate cavity (channel IIa⁷) were minimized, with the exception that Fe and its ligands were held fixed. The internal Connolly surface was constructed by use of a 0.8 Å solvent sphere. Using a larger solvent sphere (1.4 Å) resulted in a surface that was interrupted by a few amino acid side chains (Ile⁵⁵³, Leu⁵⁶⁴) which could easily reorient to form a continuous surface, as noted before.⁷
- (17) An O₂ electrode was used to determine initial rates at constant [LA] as a function of [O₂], at pH 9.0, 20 °C. Kinetic parameters were determined by nonlinear least-squares fitting to the Michaelis–Menten equation. Rates were normalized for Fe content of the enzymes (ICP-AES).
- (18) Nelson, M. J.; Cowling, R. A.; Seitz, S. P. *Biochemistry* **1994**, *33*, 4966–4973.

Table 1. Kinetic Constants^a (pH 9.0, 20 °C) and Product Distributions (pH 10.0, 23 °C) for WT-SLO and Mutants

enzyme	k_{cat} (s ⁻¹)	$k_{\text{cat}}/K_{\text{M}}(\text{O}_2)$ ($\mu\text{M}^{-1}\text{s}^{-1}$)	% HPOD ^c			
			13(S)	13(R)	9(S)	9(R)
WT-SLO	210	4.4	95	3	<1	2
Ile ⁵⁵³ →Ala	209	6.1	97	1	<1	<1
Gln ⁴⁹⁵ →Ala	120	2.4	95	2	1	2
Ile ⁵³⁸ →Ala	110	3.2 (0.2)	93	3	2	3
Leu ⁵⁴⁶ →Ala	3.0	0.4 (0.3)	85	2	3	10
Leu ⁷⁵⁴ →Ala	0.18	>0.2 ^b	62	12	10	16
Ile ⁵⁵³ →Phe	105	0.72	95 (2)	2	1	2

^a Corrected for Fe content; see Supporting Information. Standard error is less than 15% of the parameter, unless specified in parentheses. ^b $K_{\text{M}}(\text{O}_2)$ was too low to be measured ($\leq 1 \mu\text{M}$). ^c Average of two separate experiments. The estimated error ((run 1 - run 2)/2) is less than 1, unless noted in parentheses.

Leu⁵⁴⁶ and Leu⁷⁵⁴. Such binding predicts that Gln⁴⁹⁵ and Ile⁵³⁸ will interact with C-14 and C-8 of L^{*}, respectively, which would disfavor a planar pentadienyl moiety.⁷ The side channel bordered by Ile⁵⁵³ intersects cavity IIa between Leu⁵⁴⁶ and Gln⁴⁹⁵, a position that would be occupied by C-13 of bound L^{*}. Additionally, this channel encounters the active site on the face of cavity IIa opposite that of Fe²⁺. It seems feasible that O₂ enters through this channel, reacting with substrate before encountering Fe²⁺. To test this hypothesis, the bulkiness of critical side chains near this intersection was changed by site-directed mutagenesis,^{14,15} and the characteristics of the O₂ reaction with L^{*} were compared to those of WT-SLO.

Table 1 contains a summary of kinetic data¹⁷ for these mutants and WT-SLO. The overall rate of catalysis (k_{cat}) is limited by H^{*} abstraction, whereas the rate of O₂ chemistry ($k_{\text{cat}}/K_{\text{M}}(\text{O}_2)$) reflects only those steps from O₂ encounter to product release. The mutants exhibited three types of behavior, depending on how the rates of overall catalysis and of O₂ chemistry were affected by the mutation. Ile⁵⁵³→Ala has little effect on the rates of overall catalysis (k_{cat}) and oxygenation chemistry ($k_{\text{cat}}/K_{\text{M}}(\text{O}_2)$), while Gln⁴⁹⁵→Ala and Ile⁵³⁸→Ala reduce these parameters by ca. 2-fold. Leu⁵⁴⁶→Ala and Leu⁷⁵⁴→Ala greatly reduce overall catalysis (k_{cat}) decreases by ca. 100–1000-fold), while having a lesser effect on oxygenation chemistry. Finally, Ile⁵⁵³→Phe is interesting in that it greatly reduces the rate of oxygenation chemistry relative to WT-SLO and Ile⁵⁵³→Ala, while leaving k_{cat} relatively unchanged. This suggests that Ile⁵⁵³→Phe impedes O₂ access to the carbon radical intermediate (L^{*}), and supports the view that O₂ enters the active site through the channel that passes residue 553.

The radical intermediate L^{*} has generally been depicted as a pentadienyl radical, in which radical character is spread over C-9–C-13, generating greater stability than for an allyl radical. This would make C-9 and C-13 equally reactive to O₂ attack, barring accessibility differences. However, the side chains of Ile⁵³⁸ and Gln⁴⁹⁵ provide sufficient bulk to disfavor the planar pentadienyl intermediate,⁷ raising the possibility that L^{*} is an ene-allyl radical. If the unpaired electron density of L^{*} were localized near C-13, in the form of a Δ^9 -[11,12,13] allyl radical, then O₂ would be expected to selectively react at C-13. However, an EPR investigation into the identity of L^{*} showed predominantly a Δ^{12} -[9,10,11] ene-allyl radical,¹⁸ suggesting that radical character is localized

near C-9. The Gln⁴⁹⁵→Ala and Ile⁵³⁸→Ala mutations should each reduce the amount of strain that might favor a localized ene-allyl radical. However, these mutations had only modest effects on the rate of oxygenation, suggesting that such an ene-allyl radical is not formed during turnover, or else that there is rapid interconversion between the Δ^{12} -[9,10,11] and Δ^9 -[11,12,13] radicals. Additionally, these mutants produce the same product distribution as WT-SLO (*vide infra*).

Table 1 lists the stereo- and regiochemical product distributions for each enzyme, as determined by chiral HPLC analysis.^{19,20} It is immediately apparent that the dominant product for WT-SLO is 13-(S)-HPOD, with trace amounts of 13-(R), 9-(S), and 9-(R) isomers. This product distribution is observed for all other mutants, except for Leu⁵⁴⁶→Ala and Leu⁷⁵⁴→Ala. Both of these mutants replace a bulky Leu side chain with that of Ala at the constriction within the substrate cavity. It is noteworthy that Leu⁵⁴⁶→Ala yields 13-(S)- and 9-(R)-HPOD, the stereoisomers formed by addition of O₂ on the same face of L^{*}; inverse (head-to-tail) substrate binding would yield the 9-(S) isomer.⁶ Leu⁷⁵⁴→Ala yields an increase not only in the 9-(R) isomer, but also a similar increase in the 13-(R) and 9-(S) isomers, with ca. 3% of the all-trans-HPOD isomers formed as well (supplementary material). The reasons for the formation of these other isomers are unclear, but Leu⁷⁵⁴ does sit roughly adjacent to the Fe³⁺-OH, and removal of this bulky side chain could easily permit the LA substrate to adopt alternative binding modes. These data indicate that the constriction in cavity IIa formed by Leu⁵⁴⁶ and Leu⁷⁵⁴ sterically prevents O₂ access to the C-9 position within the putative pentadienyl radical, thereby imparting regioselectivity to this reaction. This obviates any requirement for the (Fe-OOL)²⁺ intermediate during turnover, suggesting that purple lipoyxygenase is not catalytically relevant.

These results present a departure from typical views of substrate-activating oxygenases, in that O₂ has seldom been thought to require a discrete and separate access channel. The present analysis shows how simple sterics can control the reaction of an enzyme-bound radical with O₂, and it provides a structural rationale for product distributions within the lipoyxygenase family. Other substrate-activating oxygenases,^{21,22} such as the cofactor-generating activity of TOPA-containing amine oxidase,²³ may also sterically direct O₂ attack to a specific site of the substrate, thereby controlling product identity.

Acknowledgment. We thank Professor T. Holman (UCSC) for providing the Q495A mutant plasmid. We thank the Swiss National Foundation and the NIH (GM25765, F32-GM19843) for funding.

Supporting Information Available: Chromatograms showing peak assignments and a table listing Fe content of each enzyme (PDF). This material is available free of charge via the Internet at <http://pubs.acs.org>.

JA003855K

- (19) Martini, D.; Iacazio, G. *J. Chromatogr. A* **1997**, *790*, 235–241.
 (20) Lopez-Nicolas, J. M.; Perez-Gilbert, M.; Garcia-Carmona, F. *J. Chromatogr. A* **1999**, *859*, 107–111.
 (21) Orville, A. M.; Lipscomb, J. D.; Ohlendorf, D. H. *Biochemistry* **1997**, *36*, 10052–10066.
 (22) Stubbe, J.; vanderDonk, W. A. *Chem. Rev.* **1998**, *98*, 705–762.
 (23) Dove, J. E.; Schwartz, B.; Williams, N. K.; Klinman, J. P. *Biochemistry* **2000**, *39*, 3690–3698.